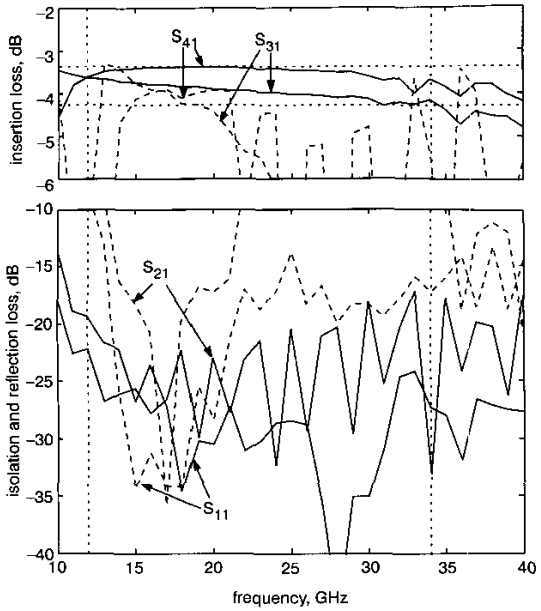

Fig. 3 *Predicted performance of dual-ferrite FCL and single-ferrite FCL*
– – – dual-ferrite FCL
----- single-ferrite FCL

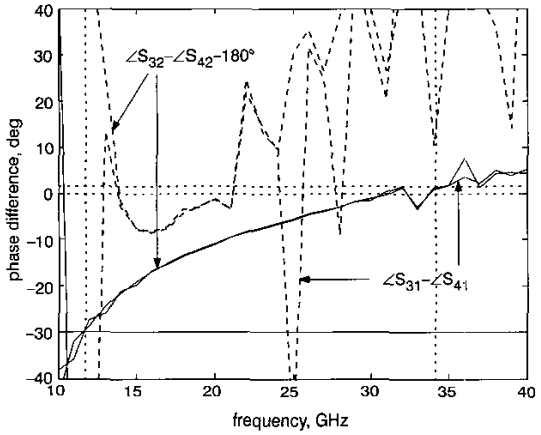

Fig. 4 *Phase behaviour of* $(\angle S_{31}-\angle S_{41})$ *and* $(\angle S_{32}-\angle S_{42}-180°)$ *for dual-ferrite FCL and single-ferrite FCL*
– – – dual-ferrite FCL
----- single-ferrite FCL

Predicted results: A dual-ferrite stripline coupled line structure with $w = 0.3$ mm, $S = 0.6$ mm and $d_1 = d_2 = 0.635$ mm, is considered. The relative permittivity and saturation magnetisation of the ferrite are $\varepsilon_f = 13$ and $M_s = 239$ kA/m ($4\pi M_s = 3000$ G), respectively. Computation using FEM shows that the optimum length for such a structure is 16.1 mm. This structure is then simulated using Ansoft HFSS assuming copper conductivity $\sigma = 5.7 \times 10^7$ S/m and the dielectric loss tangent of the ferrite, $\tan\delta = 0.002$. Fig. 2 shows the electric field outputs at ports 3 and 4 of the FCL structure when a signal is fed into port 1. With reference to port numbering in Fig. 2, Fig. 3 shows the simulated performance of the FCL between 12 to 34 GHz. Over the frequency range 12–34 GHz, S_{31} and S_{41} are between −3.4 dB to −4.2 dB and the reflection loss and isolation are below −18 dB. If the perfect conduction and $\tan\delta = 0$ are assumed, S_{31} and S_{41} are between −2.8 and −3.2 (−3 dB being ideal). The performance of this structure is compared to that of a practical single-ferrite FCL which has the following parameters: $w = 0.3$ mm, $S = 0.6$ mm and $d_1 = d_2 = 0.635$ mm, $M_s = 239$ kA/m, $\varepsilon_f = 13$ (region II), relative permittivity of dielectric $\varepsilon_r = 10.2$ (region I), $\tan\delta = 0.002$ for both ferrite and dielectric, and with an optimum operating length of 30 mm. Fig. 3 clearly shows that the single-ferrite FCL has a much narrower bandwidth, between 15 to 20 GHz (about 30% of the centre frequency). Within this bandwidth, the insertion loss S_{31} and S_{41} are between −3.9 to −4.4 dB and the reflection loss and isolation are below −17 dB. Assuming power is fed into port 1 only, the power loss P_{Loss} (%) in the FCL structure can be calculated by:

$$P_{loss} = (1 - |S_{21}|^2 - |S_{31}|^2 - |S_{41}|^2) \times 100\% \quad (2)$$

At 16 GHz, the calculated power losses (due to the conductors and dielectric only) in the dual-ferrite and the single-ferrite structures are 11.8% (0.55 dB) and 18.3% (0.88 dB), respectively. Comparatively, the power loss in a dual-ferrite FCL is 36% less than that in the conventional single-ferrite FCL. The phase characteristics of the dual-ferrite structure are shown in Fig. 4. Within the bandwidth, the values of $(\angle S_{31} - \angle S_{41})$ and $(\angle S_{32} - \angle S_{42} - 180°)$ are virtually identical and are between −30° to 2°. Compared to the single-ferrite structure, these phase characteristics are less sensitive to frequency variation, and this is important for its broad bandwidth characteristics.

Conclusion: Computed results indicate that the length of an FCL structure can be approximately halved by using a dual-ferrite structure magnetised in anti-parallel directions. This in turn leads to reduced conductor and dielectric losses. In addition, the results indicate that bandwidths of approximately 3:1 may be achievable. It may be possible to fabricate dual-magnetisation FCLs using latched ferrite toroids or high-anisotropy ferrites.

18 January 2003
Electronics Letters Online No: 20030289
DOI: 10.1049/el:20030289

C.K. Queck and L.E. Davis (*The Electromagnetics Centre for Microwave and Millimetre-Wave Design and Applications, Department of Electrical Engineering and Electronics, University of Manchester Institute of Science and Technology, P.O. Box 88, Manchester M60 1QD, United Kingdom*)

E-mail: mchpicq2@stud.umist.ac.uk

References

1 TEOH, C.S., and DAVIS, L.E.: 'Design and measurement of microstrip ferrite coupled line circulators', *Int. J. RF Microw. Comput. Aided Eng.*, 2001, **11**, (3), pp. 121–130
2 QUECK, C.K., DAVIS, L.E., XIE, K., NEWSOME, K., CLIMER, B., and PRIESTLEY, N.E.: 'Performance of stripline-type FCL circulators', *Int. J. RF Microw. Comput. Aided Eng.* (accepted)
3 QUECK, C.K., and DAVIS, L.E.: 'Microstrip and stripline ferrite-coupled-line (FCL) circulators', *IEEE Trans. Microw. Theory Tech.*, 2002, **50**, (12), pp. 2910–2917
4 XIE, K., and DAVIS, L.E.: 'Nonreciprocity and the optimum operation of ferrite coupled lines', *IEEE Trans. Microw. Theory Tech.*, 2000, **48**, (4), pp. 562–573
5 XIE, K., and DAVIS, L.E.: 'Performance of axially-magnetized ferrite coupled lines', *Radio Sci.*, 2001, **36**, (6), pp. 1353–1362
6 MAZUR, J., and MROZOWSKI, M.: 'On the mode coupling in longitudinally magnetized waveguiding structures', *IEEE Trans. Microw. Theory Tech.*, 1989, **37**, (1), pp. 159–164

Frequency tuning in electromagnetic bandgap nonlinear transmission lines

F. Martín, J.L. Carreras, J. Bonache, F. Falcone, T. Lopetegi, M.A.G. Laso and M. Sorolla

Frequency tuning in stopband filters based on nonlinear transmission lines is demonstrated for the first time. The structure is an electromagnetic bandgap (EBG) coplanar waveguide reflector periodically loaded with varactor diodes, acting as tuning elements. By varying the capacitance of the diodes the phase velocity can be tailored, the result being a wide tuning range for the central frequency of the rejected band. It was also found that the EBG-based reflector is able to inhibit harmonic generation under large-signal driving conditions.

Introduction: Nonlinear transmission lines (NLTLs) are high impedance transmission media periodically loaded with shunt connected nonlinear devices, such as Schottky or heterostructure varactor diodes. These structures have been usually fabricated in coplanar waveguide (CPW) technology because no vias are required for nonlinear device grounding and this eases fabrication. Owing to their periodicity, NLTLs are dispersive structures which exhibit passband-stopband characteristics, the first passband being delimited by the Bragg frequency. Below this frequency, the propagation velocity can be approximated by $v_p = l/[L(C + C_{ls})]^{1/2}$, where L and C are the per-section inductance and capacitance of the unloaded line. C_{ls} is the large signal capacitance of the diodes (defined as the average value under large-signal conditions), or the quiescent capacitance in the linear regime, and l is the distance between adjacent diodes. According to the previous expression, the presence of capacitors decreases the phase velocity of the line. The resulting structure exhibits therefore a slow wave effect which is of interest for the design of compact devices.

In recent years, CPW NLTLs have been used for the design of compact lowpass filters [1] and time delay phase shifters [2] (linear conditions). Under large-signal conditions, device nonlinearity combined with dispersion has been applied to the design of picosecond pulse generators and frequency multipliers [3, 4]. However, the possibility to control propagation velocity by properly biasing varactor diodes, opens the door to the design of tunable devices such as filters or resonators. In this Letter, a tunable stopband filter based on the reflection properties of an electromagnetic bandgap (EBG) structure is proposed. An EBG [5] is essentially a transmission line with periodic perturbations of wave impedance (or effective permittivity) around a nominal value. Owing to this impedance modulation, signal propagation is inhibited in a frequency band the central frequency of which, f_o, is related to the period of the perturbation, λ_T, by $f_o = v_p/2\lambda_T$ (Bragg condition). If the propagation velocity, v_p, can be tailored by means of an external bias, frequency tuning can thus be achieved. Therefore, by combining an EBG reflector with an NLTL, a tunable band stop filter can potentially be obtained. Based on this new idea, a CPW with shunt connected varactor diodes and periodically perturbed by varying the slot width, has been designed and fabricated. As will be shown, the fabricated structure exhibits a wide tuning range exceeding 35%.

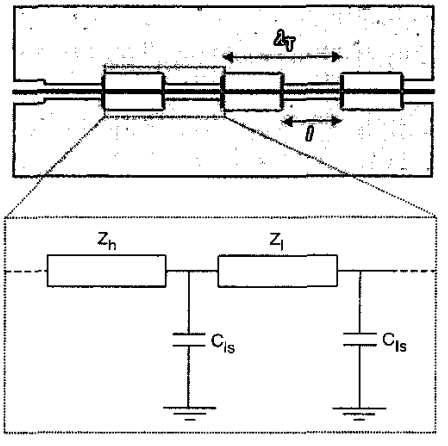

Fig. 1 *Typical layout of EBG-NLTL and schematic diagram of basic cell*
Shunt connected varactors represented by black rectangles placed in the layout steps

Design of EBG-NLTL tunable filter: Fig. 1 shows a typical layout of an EBG-NLTL structure, where varactor diodes are disposed in parallel pairs, and wave impedance modulation is implemented by varying the distance between the central strip (of constant width) and ground planes. The design of the structure requires the determination of l, λ_T, the lateral dimensions of the high/low impedance sections of the CPW and the choice of suitable varactor diodes. To achieve a wide tuning range, it is necessary that the capacitance of the diodes dominates over the per-section capacitance of the unloaded line (i.e. $C_{ls} > C$). However, to avoid significant mismatches, it is convenient that the characteristic impedance of the NLTL including the presence of diodes (or Bloch impedance)

$$Z_L = \sqrt{\frac{L}{C + C_{ls}}} \tag{1}$$

is as close as possible to $Z_L = 50\,\Omega$ in the whole tuning range. Finally, the cutoff (Bragg) frequency of the NLTL

$$f_B = \frac{1}{\pi\sqrt{L(C + C_{ls})}} \tag{2}$$

which is also dependent on the bias point of varactor diodes, must be sufficiently separated from f_o to ensure that the rejected band of the structure lies below cutoff.

BB833-Infineon Technologies silicon tuning diodes have been used as nonlinear elements. These devices exhibit a high capacitance ratio which is of interest to achieve a wide tuning range (device capacitance is 9 pF and 0.75 pF at 1 and 28 V reverse bias, respectively). By separating the diodes a distance $l = 34$ mm and setting the conductor strip and slot widths to $W = 1.6$ mm and $G = 4$ mm, respectively, the characteristic impedance and Bragg frequency of the unperturbed CPW are nominally $Z_L = 50\,\Omega$ and $f_B = 0.75$ GHz, respectively, for 5 V reverse biased diodes. These geometric parameters have been obtained by inverting (1) and (2) and the use of a commercial transmission line calculator (the parameters of the Rogers RO3010 substrate have been considered, i.e. $\varepsilon_r = 10.2$, thickness $h = 1.27$ mm). The impedance of the unloaded line is found to be $Z_o = (L/C)^{1/2} = 104\,\Omega$. To complete the design of the structure, it is necessary to determine the period and magnitude of the perturbation. The former determines the central frequency of the rejected band, while the latter is related to the level of attenuation. For the fabrication of the prototype, the period of the perturbation has been set to $\lambda_T = 2l$ (as in Fig. 1). With this choice, a frequency gap is expected to be opened near the cutoff frequency since, following the Bragg condition, the electrical length is $\beta l = \pi/2$ at f_o. According to the dispersion relation [6]:

$$\cos\beta l = \cos(2\pi f\sqrt{LC}) - \frac{2\pi f C_{ls} Z_o}{2}\sin(2\pi f\sqrt{LC}) \tag{3}$$

This corresponds to a frequency in the vicinity of f_B. To achieve significant rejection level in the stopband of the filter, step variations of 40 Ω up and down Z_o have been considered. This wave impedance modulation is obtained by alternating the slot width between $G = 8.3$ mm (high impedance sections, Z_h) and $G = 1.3$ mm (low impedance sections, Z_l). A ten capacitor-stage prototype has been fabricated with these parameters.

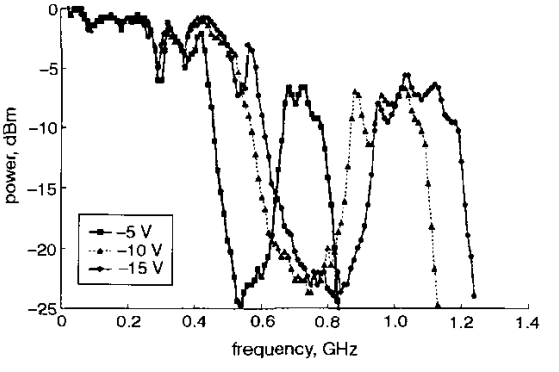

Fig. 2 *Measured frequency responses for fabricated EBG-NLTL with diodes biased at different reverse voltages*

Results: The characterisation of the fabricated EBG-NLTL structure has been carried out by means of an E4438C Agilent Technologies microwave power source and Tektronix 2711 spectrum analyser. Fig. 2 shows the linear frequency response (0 dBm feeding signal) for the diodes reverse biased at 5, 10 and 15 V. As expected, a tunable frequency gap arises near cutoff. The lower sensitivity of the central frequency at high diode voltages is a consequence of the lower degree of nonlinearity for the loading devices. Nevertheless, a wide tuning range has been achieved for control voltages varying between 5 and

15 V, namely $\Delta f_o/f_{central} \simeq 35\%$, where $f_{central}$ is the central frequency of the swept interval (Δf_o). Measurements under large signal conditions have also been carried out to check the ability of the structure to inhibit harmonic generation in the bandgap. For this, the power of the driving signal has been set to 22 dBm and the output power for the fundamental, second- and third-harmonics has been measured. The results are shown in Fig. 3, where clearly the reflection properties of the EBG-NLTL are also manifested under nonlinear conditions. This is not evident since harmonics are generated during propagation and their phase does not vary linearly with position.

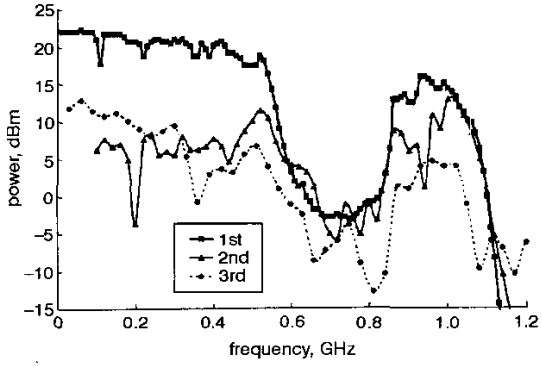

Fig. 3 *Nonlinear measurements for fabricated prototype with diodes reverse biased at 10 V*

For second- and third-harmonics, x-axis is frequency of that harmonic (not the fundamental)

Conclusion: Frequency tuning in EBG-NLTLs has been demonstrated for the first time. Specifically, a tunable stopband filter based on the reflection properties of a stepped impedance EBG-NLTL has been fabricated in CPW technology. Linear and nonlinear measurements have demonstrated a wide tuning range and the capability of the structure to inhibit the generation of harmonics lying in the frequency gap. Owing to capacitive coupling, the structure also exhibits slow wave effects which are of interest for the reduction of device dimensions. This work opens the door to the design of compact tunable devices based on the combination of NLTLs with EBGs and other distributed structures.

Acknowledgments: This work has been supported by DGI and CICYT through project contracts BFM2001-2001 and TIC2002-04528-C02-01. The authors thank the DURSI (Generalitat de Catalunya) for supporting this work by means of an ACI Action ACI2001-33. They thank D. Gonzalo (Agilent Technologies) for lending the microwave source.

13 December 2002
Electronics Letters Online No: 20030307
DOI: 10.1049/el:20030307

F. Martín, J.L. Carreras and J. Bonache (*Departament d'Enginyeria Electrònica, Universitat Autònoma de Barcelona, 08193 Bellaterra (Barcelona), Spain*)

F. Falcone, T. Lopetegi, M.A.G. Laso and M. Sorolla (*Departamento de Ingeniería Eléctrica y Electrónica, Universidad Pública de Navarra, 31006 Pamplona, Spain*)

References

1 MARTIN, F., FALCONE, F., BONACHE, J., LOPETEGI, T., LASO, M.A.G., and SOROLLA, M.: 'New periodic-loaded electromagnetic bandgap coplanar waveguide with complete spurious passband suppression', *IEEE Microw. Wirel. Compon. Lett.*, 2002, **12**, (11), pp. 435–437

2 YONEDA, H., TOKUYAMA, K., UEDA, K., YAMAMOTO, H., and BABA, K.: 'High power terahertz radiation with diamond photoconductive antenna array' *in* LUI, S. and SHEN, X. (Eds.): 25th Int. Conf. on Infrared and Millimeter Waves Conf. Dig., Beijing, People's Republic of China, September 2000 p. 61

3 RODWELL, M.J.W., ALLEN, S.T., YU, R.Y., CASE, M.G., BHATTACHARYA, U., REDDY, M., CARMAN, E., KAMEGAWA, M., KONISHI, Y., PUSL, J., and PULLELA, R.: 'Active and nonlinear wave propagation devices in ultrafast electronics and optoelectronics', *Proc. IEEE*, 1994, **82**, pp. 1037–1059

4 FERNANDEZ, M., DELOS, E., MELIQUE, X., ARSCOTT, S., and LIPPENS, D.: 'Monolithic coplanar transmission lines loaded by heterostructure barrier varactors for a 60 GHz tripler', *IEEE Microw. Wirel. Compon. Lett.*, 2001, **11**, pp. 498–500

5 YANG, F.R., MA, K.P., QIAN, Y., and ITOH, T.: 'A uniplanar compact photonic bandgap structure and its applications for microwave circuits', *IEEE Trans, Microw. Theory Tech.*, 1999, **47**, pp. 1509–1514

6 POZAR, D.M.: 'Microwave engineering' (Addison Wesley, Reading, MA, 1990)

Phase noise characterisation of planar magnetostatic wave oscillators

G. Bartolucci, R. Marcelli and Jinsong Chen

The phase noise performances of a planar configuration of a magnetostatic wave oscillator have been investigated. The behaviour of the output signal has been studied in terms of the single sideband power spectral density. Values as low as −100 dBc at 100 kHz of offset from the carrier frequency have been measured in the whole range of tunability, by using two different resonators.

Introduction: Microwave oscillators are widely used in many high frequency equipments and telecommunication systems. Very important requirements in the design and realisation of sinusoidal oscillators concern the spectral purity of the output signal. A conventional representation of the spectral purity is the so called 'single sideband noise power spectral density', or $L(f_m)$, defined as the ratio of the noise power in one sideband at an offset frequency f_m from the carrier, with respect to the power of the carrier [1]. A microwave oscillator is essentially composed of an active device, a passive resonator, and a matching circuit to the external load. To improve the phase noise performances of this component (i.e. to obtain low values for $L(f_m)$), two strategies are followed: (i) the choice of a semiconductor element with very low $1/f$ noise; (ii) the increase of the Q factor of the resonator. Therefore, when the active element has been chosen between those commercially available, the second method is pursued. For this purpose, dielectric and magnetic resonators are currently utilised. The latter exhibit the interesting property to allow the tunability of the oscillation frequency, obtained by changing the DC bias magnetic field. The standard realisation of this kind of oscillator requires a sphere of magnetic material [2]. In this case, the main drawback lies in the very difficult integration of the magnetostatic wave device. To solve this problem, a planar rectangular iron garnet film directly coupled to a microstrip line was proposed (e.g. [3]), and successively exploited in other configurations, e.g. the X- and Ku-band microwave oscillators given in [4–6]. Our aim in this Letter is to present the experimental characterisation of the oscillator studied in [5] in terms of the noise power spectral density.

Experimental results and discussion: The layout of the whole component, realised onto an alumina substrate with a thickness of 254 μm, is shown in Fig. 1 [5]. For the active element the HEMT NEC 32400 was chosen. The rectangular magnetic planar resonator was modelled by means of a lumped element equivalent circuit [5]. A matching network was inserted between the active device and the load, and it was designed imposing the fulfilment of the Barkhausen conditions. Two yttrium iron garnet films, with planar dimensions 2×0.8 mm^2 and 3×0.8 mm^2 and both 30 μm thick, were used for the realisation of the resonator, resulting in different oscillation frequency ranges. The experimental setup for the measurement of the power spectral density was composed of a spectrum analyser HP8656, and a DC magnetic bias structure made by two permanent magnets. By changing the position of two metal plates orthogonally positioned with respect to the direction of the DC magnetic bias field H_0 in the prototype structure, the strength of the bias field was decreased or increased, thus obtaining the frequency tunability. The behaviour of the output power of the oscillator, measured by means of the spectrum analyser, is shown in Fig. 2, for both the 2×0.8 mm^2 film and the 3×0.8 mm^2 one, against oscillation frequency. Powers not lower than